

CAD Technique for Microwave Chemistry Reactors with Energy Efficiency Optimized for Different Reactants

Ethan K. Murphy¹ and Vadim V. Yakovlev²

¹ Applied Mathematics, Inc., Gales Ferry, CT 06335, USA
ethan.kane.murphy@gmail.com

² Department of Mathematical Sciences, Worcester Polytechnic Institute, Worcester, MA 01609, USA
vadim@wpi.edu

Abstract — Upgrading successful processes of microwave-assisted organic synthesis to the level of industrial technology is currently slowed by difficulties in experimental development of large-scale and highly-productive reactors. This paper proposes to address this issue by developing microwave chemistry reactors as microwave systems, rather than as black-box-type units for chemical reactions. We suggest an approach based on the application of a neural network optimization technique to a microwave system in order to improve its coupling (and thus energy efficiency). The RBF network optimization with CORS sampling introduced in our earlier work and capable of exceptionally quick convergence to the optima due to a dramatically reduced number of underlying 3D FDTD analyses, is upgraded here to account for an additional practically important condition requiring optimal design of the reactor for different reactants. Viability of the approach is illustrated by three examples of finding the geometry of a conventional 99% energy efficient microwave reactor for 3/3/6 different materials; with 1/5/1 liter reactants, seven-parameter optimization yields the best configurations taking only 16/38/115 hours of CPU time of a regular PC.

Index Terms — FDTD simulation, microwave reactor, neural network, optimization, scaling up.

I. INTRODUCTION

Microwave (MW)-assisted organic synthesis (MAOS) has recently become a frontline methodo-

logy in chemistry programs of pharmaceutical, agrochemical, and biotechnology industries due to its ability to significantly speed up chemical reactions [1-3]. With specialized systems for MW chemistry now available, particular attention is currently paid to the problem of development of controlled MAOS featuring new reaction routes for organic synthesis resulting in large-scale production of chemical substances [3]. In order for MAOS to become a widely accepted industrial technology, there is a need to develop techniques routinely producing new chemical entities on a scale of dozens/hundreds of kilograms. However, surveying the contemporary literature, one may notice that progress in this direction is fairly slow. While scaling up successful processes of MW chemistry is commonly acknowledged to be a key issue of the current state of the field, this problem is being addressed via essentially trial-and-error experiments aiming, with no way to measure the temperature inside the reactant, to catch correlation between the input parameters of the scaled up MW reactors and the output chemical characteristics of the products [4].

Comprehensive modeling of interactions of the reactants with the electromagnetic field in closed systems appears to be a powerful tool applicable to the MW chemistry reactors. Specifically, modeling can be used for determining reflections (i.e., for finding energy efficiency of the reactors) as well as spatial distributions of dissipated power in the reactant; application of an appropriate computational procedure to MW systems suitable for MAOS is exemplified, e.g., in [5]. There are also electromagnetic modeling techniques that compute

temperature fields in the processed materials by taking into account thermal dependence of material parameters [6]. Some multiphysics computational technologies couple electromagnetic and thermodynamic simulations of heated materials with temperature-dependent electromagnetic and thermal material parameters [7, 8]. Moreover, there are modeling-based procedures that optimize MW applicators for energy efficiency [9] and synthesize optimal processes, resulting in homogeneous temperature fields [10, 11]. Despite being known and used in other MW power applications, these advanced computational approaches seem to not be utilized in microwave chemistry. Examples of employing computer simulation in design of MAOS reactors as MW systems are rare [12, 13] and limited to insufficiently accurate analysis (rather than optimization or synthesis) of the reactor's operational regimes.

Computational schemes using neural network techniques and allowing for direct designing MW devices (by providing the system geometry for a given electromagnetic specification) have been described in [14-17]. In this paper, we present an original technique for direct computer-aided design (CAD) of MW reactors of a desirable scale and sufficiently high energy efficiency to process different reactants. The approach is based on the radial basis function (RBF) network optimization algorithm originally introduced in [14] and principally upgraded in [16], featuring

- (i) an objective function (OF) measuring the bandwidth of the frequency characteristic of the reflection coefficient over a specified frequency range and
- (ii) the constrained optimization response surface (CORS) technique [18] selecting additional sample points in the dynamic training of the network.

This algorithm, backed by 3D FDTD data, is characterized by very quick convergence to the optima and a dramatic reduction in the required number of underlying analyses. Due to these features, it has strong potential for viable optimization of complex MW systems and/or structures with a large number of design variables.

Here, the technique [16] is upgraded by incorporating an additional practically important condition requiring optimality of the reflection coefficient for different processed materials. Functionality

of the resulting algorithm is illustrated by finding the optimal designs of a conventional reactor containing vessels with 1 and 5 liter reactants. It is shown that for finding the best configurations of the system (suitable for three and six different reactants) from seven-parameter optimizations, only a few dozen/hundred simulations are required.

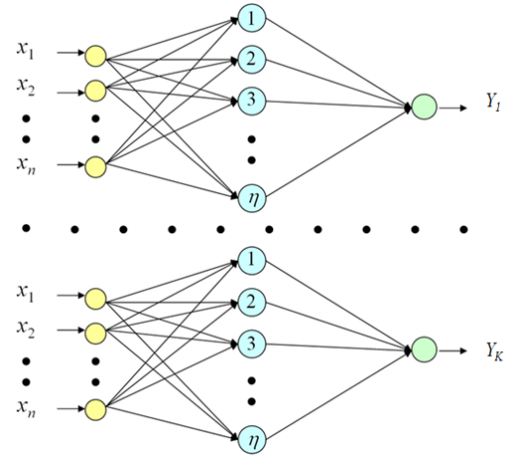


Fig. 1. Architecture of a decomposed RBF ANN with η hidden neuron [14, 16].

II. OPTIMIZATION TECHNIQUE: RBF NETWORK AND OBJECTIVE FUNCTIONS

In accordance with [16], the decomposed RBF artificial neural network (ANN) shown in Fig. 1 and denoted as $F: X \rightarrow Y$ works with input vectors $X_i = [x_1 \ x_2 \ \dots \ x_N]$, where x_1, \dots, x_N are design variables for $i = 1, \dots, P$, and P is the number of input-output pairs of modeling data. In the upgraded version of the algorithm proposed in this paper, the network output is obtained by taking frequency characteristics of an S -parameter over specified frequency range(s) (f_1, f_2) given by the formula

$$Y_i = \max_{1 \leq k \leq L} [BW_r(S_k, T) + 1]^{-1}, \quad (1)$$

where

$$S_k = S(f_1 \leq f \leq f_2, X_i, \varepsilon'_k, \sigma_k),$$

and T is the tolerance defined for the j th frequency interval. The function BW_r (associated with the system's bandwidth BW) is calculated over the

specified frequency interval and outputs relative bandwidth in the range $[0, 1]$, and L is the number

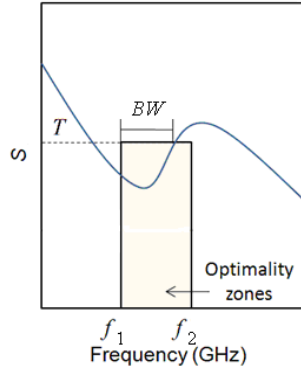


Fig. 2. Parameters of objective function (1) with S representing S_{11} .

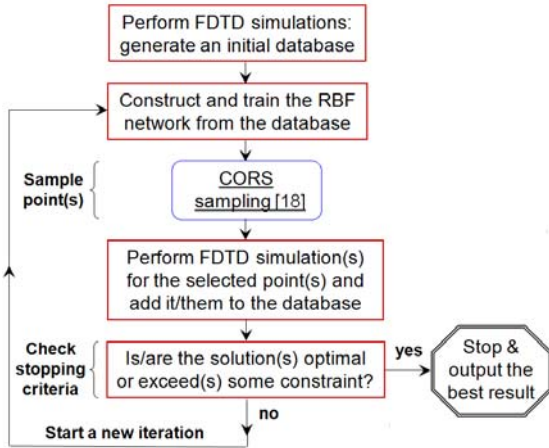


Fig. 3. RBF network optimization algorithm with CORS sampling.

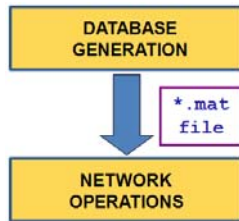


Fig. 4. Modules of the algorithm's MATLAB implementation.

of materials for which the system is to be optimized; we maximize over k to use the worst of the L samples with the dielectric constant ϵ' and electric conductivity σ . This OF represents a typical practical need of MW optimization to search not just the minimum of S , but rather the

maximum BW_r in a certain frequency range (as illustrated in Fig. 2). Motivations for the choice of the shape of the optimality zone (i.e., the values of f_1 , f_2 , and T) for problems of MW power engineering are discussed in [9]. The RBF used in the network is a thin plate spline defined as

$$\varphi_l^{(i)} = \begin{cases} \|X_i - c_l\|_2^2 \log(\|X_i - c_l\|_2), & \|X_i - c_l\|_2 > 0, \\ 0, & \|X_i - c_l\|_2 = 0, \end{cases} \quad (2)$$

where $l = 1, \dots, N_c$, N_c is the number of RBFs, c_l are the centers of $\varphi_l^{(i)}$. The training set is the set of centers chosen. The network is coupled with a linear model, and the weights are constructed by solving the corresponding linear system.

A brief general description of the algorithm is given by the flow chart in Fig. 3. Given some initial data, we construct and train the RBF network $F(X)$, perform CORS sampling, simulate the sampled point, check stopping criteria, and repeat the cycle, if necessary. The critical part of the algorithm is the choice of additional points: CORS sampling balances the goal of finding the minimum with exploring unknown regions of the domain [18]. This is accomplished by selecting a parameter β ($0 \leq \beta \leq 1$) and finding the minimum of $F(X)$, subject to $\|X - X_i\| \geq \beta\Delta$ for $1 \leq i \leq P$, where $\Delta = \max_X(\min_{1 \leq i \leq P}\|X - X_i\|)$. The Δ is approximated by picking the maximum from a random sampling of points in the domain. This seems to be sufficient because the aim of Δ is to measure the spacing of points in the current database. In other words, the algorithm searches for minima forced away from previously sampled points based on the percentage (or fraction) given by β .

The stopping criteria chosen to be a set maximum number of database points are applied if the solution has 100% BW_r or some lower predefined value.

III. COMPUTER IMPLEMENTATION

The option of RBF network optimization for a number of different materials that is formulated in the OF (1) has been realized in this work as an upgraded MATLAB code implementing the algorithm [16].

Data for the network are generated by an FDTD model of a MW device; with an appropria-

tely applied pulse excitation, the model produces frequency responses of S -parameters. In our implementation, the data is produced with the use of the 3D conformal FDTD simulator *QuickWave-3D*

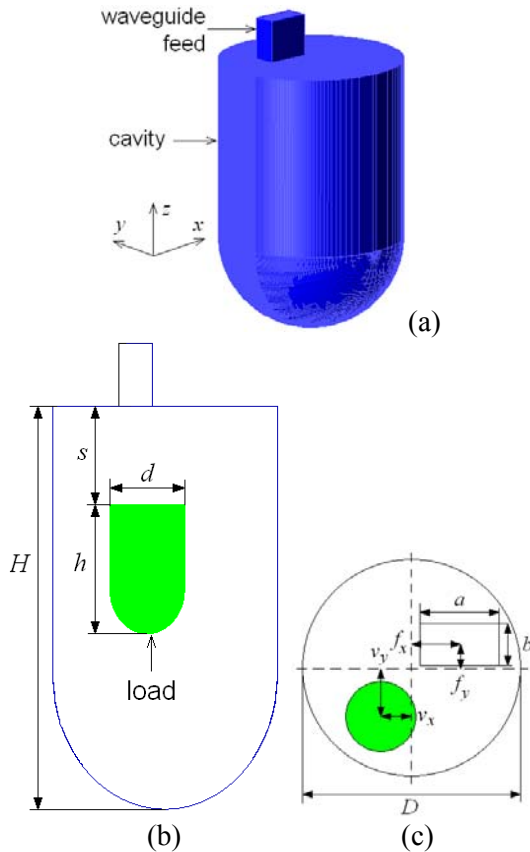


Fig. 5. General 3D view (a) and geometrical parameters of the considered reactor (b), (c).

(*QW-3D*) [19]; all CPU times are given below for a 64-bit Windows XP Intel Xeon 3.2-GHz PC.

The code consists of two modules as shown in Fig. 4. Database Generation calls *QW-3D* and constructs an initial database (DB) for the specified optimization problem and stopping criteria. This module produces a problem-specific mat-file which is then used as input data for network operations. The latter module runs optimization iterations for the chosen/specified OF, sampling technique, and RBF.

IV. NUMERICAL RESULTS: A MAOS REACTOR OPTIMIZED FOR DIFFERENT REACTANTS

Here, we consider a MW system resembling the shape of a typical MAOS reactor (Fig. 5). The

cavity is constructed by combining a hemisphere and cylinder. Inside the cavity, there is a thin-wall hemisphere-bottom cylindrical vessel with a liquid reactant whose volume V is assumed to be speci-

Table 1: Material parameters of the reactants at 2.45 GHz (adapted from [1]).

Reactant	Dielectric constant, ϵ'	Electric conductivity, σ (S/m)
(A) Ethyl acetate	6.2	0.1468
(B) Methylene chloride	9.1	0.0582
(C) Acetone	20.6	0.1178
(D) Ethanol	24.6	0.1808
(E) Methanol	32.7	4.1882
(F) Acetonitrile	36.0	3.2291

fied. The reactor is excited by a rectangular waveguide which may be offset in the x - and y -directions by f_x and f_y , respectively. The vessel also may be offset from the z -axis by v_x and v_y , and is located a distance s from the top of the cavity. The CAD goal is: given the height of the system H and a set of L reactants to be processed in the reactor, find the configuration of the whole system, i.e., diameter D , internal dimensions of the vessel (d and h), its position in the cavity (s , v_x and v_y), and a position of the waveguide (f_x and f_y), that yields less than T % of reflected microwave energy (i.e., the reflection coefficient $|S_{11}| < 0.1\sqrt{T}$) in BW_r^k % ($k = 1, \dots, L$) of the frequency range (f_1, f_2) for reactants A, \dots, L , respectively.

A. One liter load and three reactants

In the first illustration, we solve this problem for a load of $V = 1$ liter and with the height of the reactor $H = 300$ mm. We consider $L = 3$ (the materials (A), (B), and (D) specified in Table 1), $T = 1$ % (i.e., energy efficiency 99 %), $BW_r^A = \dots = BW_r^D = 100$ %, $f_1 = 2.4$ GHz, and $f_2 = 2.5$ GHz. While the waveguide dimensions are considered constant ($a = 72$ mm, $b = 36$ mm), seven design variables are allowed in the intervals:

$$\begin{aligned} -35 \leq f_x, f_y \leq 35 \text{ mm}, \quad -24 \leq v_x, v_y \leq 24 \text{ mm}, \\ 80 \leq d \leq 110 \text{ mm}, \quad 75 \leq s \leq 110 \text{ mm}, \\ 200 \leq D \leq 300 \text{ mm}. \end{aligned} \quad (3)$$

The procedure starts with a generation of an initial DB of 50 random points in the specified domain for each of the three reactants. Aiming to keep CPU time in this illustrative optimization reasonable, the chosen underlying FDTD model is

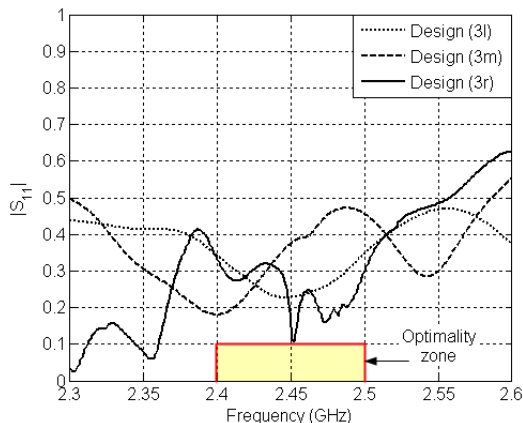


Fig. 6. Typical non-optimized characteristics of the system in Fig. 5 with Reactant (D): design variables chosen at the left-end (Design (3l)), mid-(3m), and right-end points (3r) of the intervals (3).

Table 2: Reactor configurations optimized for reactants (A), (B), and (D)

V (liters)	1	5
f_x , mm	-23.4	75.8
f_y , mm	11.0	83.2
v_x , mm	-5.3	50.0
v_y , mm	20.0	-36.0
d , mm	108.0	164.0
s , mm	94.8	145.4
D , mm	209.0	395.2
DB size/No of FDTD analysis	99/297	65/195

relatively rough: built with a non-uniform conformal mesh, it consists of 308,000 to 555,000 cells with size ranging from a maximum of 2.7 mm in the reactant to 7 mm in air. The cell size of the load is selected for materials with high dielectric constants ((D)-(F) in Table 1) and is kept the same for the materials with low ϵ' . The analysis of the system involves 10,000 time-steps (1.7 to 3.0 min of CPU time).

Characteristics of the reflection coefficient in the non-optimized reactor computed for all the reactants yield energy efficiency of about 75-85 % (see, e.g., Fig. 6). Our optimization procedure

achieves what seems to be the “best” solution producing 99 % efficiency ($BW_r^A = 79$ %, $BW_r^B = 83$ %, and $BW_r^D = 100$ %) with $99 \times 3 = 297$ FDTD analyses (Fig. 7). Corresponding design

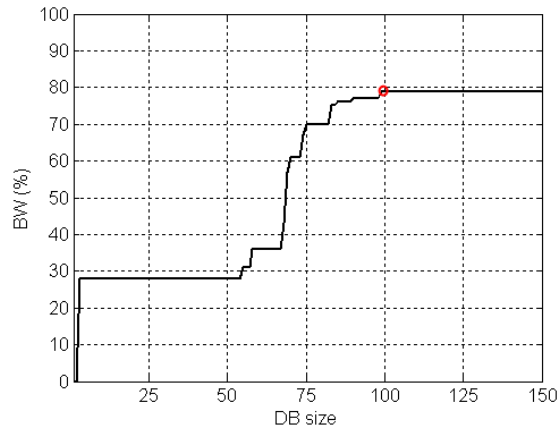


Fig. 7. Optimization convergence for the reactor designed for $T = 1\%$ and three one-liter reactants (A), (B), and (D); 99th iteration is marked by (○).

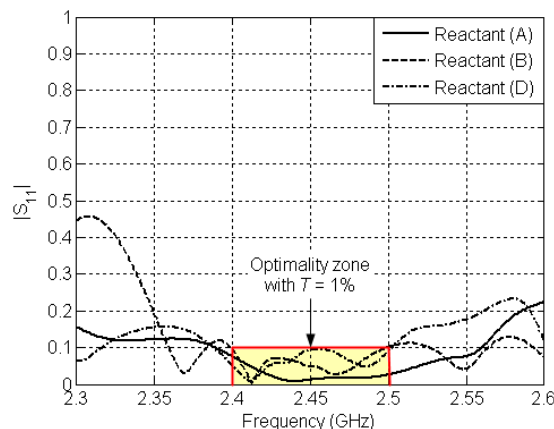


Fig. 8. Reflection coefficient in the reactor optimized for three one-liter reactants (A), (B), and (D).

variables are given in Table 2 and frequency characteristics of $|S_{11}|$ resulting from this geometry are shown in Fig. 8: it is seen that, for the reactants (A), (B), and (D), this optimized configuration provides the desirable efficiency in 79 % of the 2.4 to 2.5 GHz frequency range.

B. Five liter load and three reactants

The next example illustrates a capability of the proposed optimization technique in situations when scaling up of a successful MAOS process is

of key interest. Here, we solve the optimization problem for a reactor of the same design and constructed for the same reactants ($L = 3$), but of a 5-liter volume. With $H = 513$ mm, $T = 1$ %, $BW_r^A = \dots = BW_r^D = 90$ %, $f_1 = 2.4$ GHz, and $f_2 = 2.5$

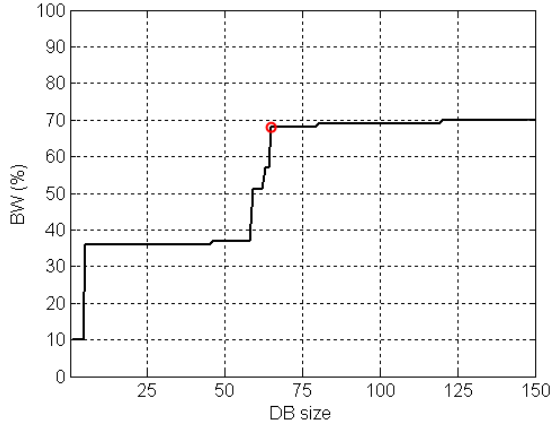


Fig. 9. Optimization convergence for the reactor designed for $T = 1$ % and three five-liter reactants (A), (B), and (D); 65th iteration is marked by (○).

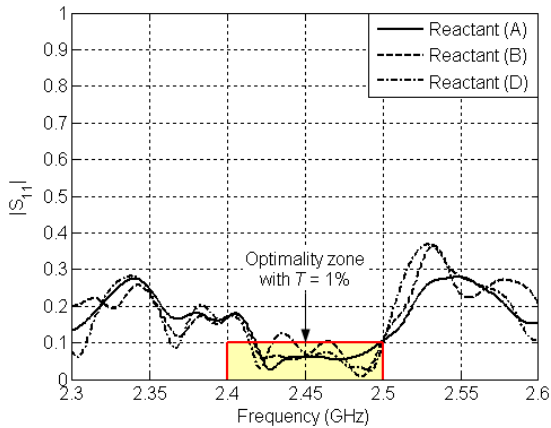


Fig. 10. Reflection coefficient in the reactor optimized for three five-liter reactants (A), (B), and (D).

GHz, the seven design variables are allowed in the intervals:

$$\begin{aligned} -85 \leq f_x, f_y \leq 85 \text{ mm}, \quad -50 \leq v_x, v_y \leq 50 \text{ mm}, \\ 159 \leq d \leq 172 \text{ mm}, \quad 80 \leq s \leq 300 \text{ mm}, \\ 340 \leq D \leq 510 \text{ mm} \end{aligned} \quad (4)$$

Similarly, the procedure starts with an initial DB of 50 random points in the domain (4). The model consists of 1,380,000 to 2,394,000 cells of maximum size 3 mm in the reactant to 7 mm in air –

due to the larger volume of the reactant, the domain discretized with 3 mm cells is also larger. Likewise, the analysis requires 10,000 time-steps (8.6 to 14.4 min of CPU time).

In the case of a 5-liter reactant, as seen from Fig. 9, the best solution ($BW_r^A = 80$ %, $BW_r^B = 77$ %, and $BW_r^C = 70$ %) is achieved with 119 DB points, but for the preceding very close result (with the worst $BW_r^C = 68$ %) the procedure needs only 65 points (195 analyses). Corresponding design variables are also given in Table 2 and $|S_{11}|$ characteristics resulting from this geometry are shown in Fig. 10: this optimized configuration provides 99 % energy efficiency for all three reactants in the 70 % of the 2.4 to 2.5 GHz frequency range.

It is seen that the optimized geometry of the 5 liter reactor is fairly different from a proportionally increased one of the 1 liter system, and the “qualities” of both best solutions are not alike. This appears to be consistent with theoretically expected (and observed in many experiments [13]) strongly non-linear alterations in a reactor’s performance with variations of its geometrical parameters and material characteristics of the reactants.

C. One liter load and six reactants

In the last illustration, the proposed CAD technique is tested with double the number of reactants ($L = 6$), i.e., all the materials specified in Table 1 and differing in a dielectric constant by about 6 times and in the conductivity by about 70 times. We assume $V = 1$ liter, $H = 300$ mm, $f_1 = 2.4$ GHz, $f_2 = 2.5$ GHz, and set the goal values $BW_r^A = \dots =$

$BW_r^F = 100$ %. The same seven design variables are allowed in the intervals given by (3). The underlying FDTD model and its CPU times are the same as in the first example above (sub-section IV.A).

First, we solve the problem for $T = 2.5$ %. The procedure starts with a generation of an initial DB of 50 points for each of the six reactants. The “best” optimal solution producing 97.5 % efficiency ($BW_r^A = \dots = BW_r^D = 100$ %, $BW_r^E = 93$ %, and $BW_r^F = 95$ %) is achieved very quickly with only 14 additional DB points; this requires a total of 384 FDTD analyses. The convergence to

this solution is illustrated in Fig. 11 for each reactant. Corresponding design variables are given in the last column of Table 3 along with the values produced from the previous 4 optimization iterations. Frequency characteristics of $|S_{11}|$ resulting from the 64th optimal solution are shown

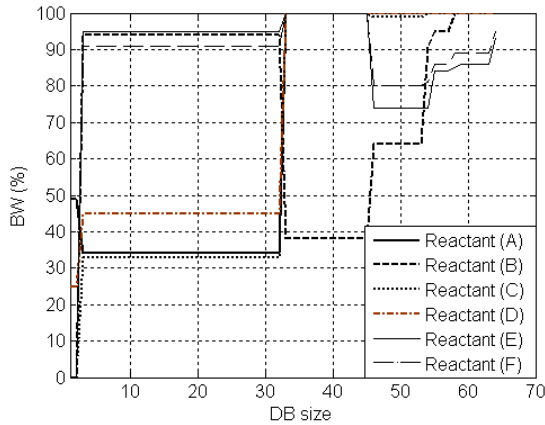


Fig. 11. Optimization convergence for the reactor designed for $T = 2.5\%$ and six one-liter reactants (A)-(F).

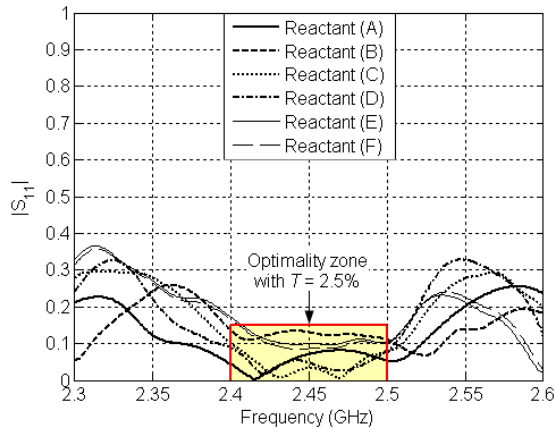


Fig.12. Reflection coefficient in the reactor optimized for six one-liter reactants (A)-(F).

Table 3: Optimal solutions of the final stage of optimization for 97.5% energy efficiency with six reactants (A)-(F).

Iter.	60	61	62	63	64
f_{x_2} , mm	-1.3	-2.6	-3.1	-2.9	-2.6
f_{y_2} , mm	-24.5	-22.1	-22.8	-22.3	-22.5
v_{x_2} , mm	-19.8	-19.6	-18.0	-18.4	-17.9
v_{y_2} , mm	-9.1	-9.0	-8.6	-8.5	-10.0
d_2 , mm	101.6	101.4	101.2	100.9	101.2
s_2 , mm	81.2	81.6	83.2	82.2	82.3
D_2 , mm	242.3	242.6	242.3	242.6	243.4

in Fig. 12: for all the reactants (A)-(F), this optimized configuration provides desirable efficiency in 93 % of the 2.4 to 2.5 GHz frequency range.

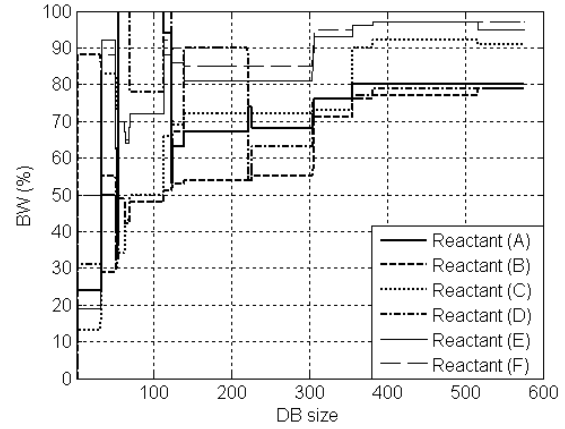


Fig. 13. Optimization convergence for the reactor designed for $T = 1\%$ and six one-liter reactants (A)-(F).

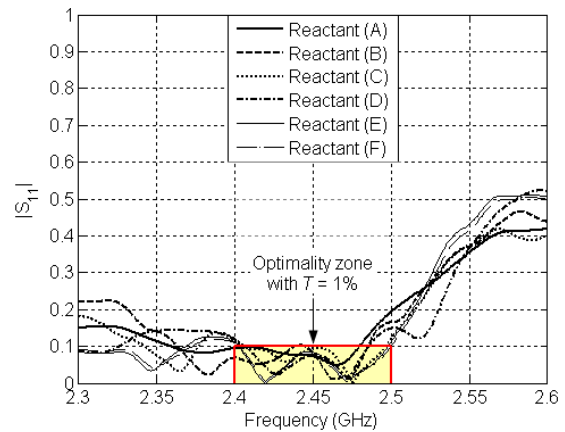


Fig. 14. Reflection coefficient in the reactor optimized for three 1-liter reactants (A)-(F).

Table 4: Optimal solutions of the final stage of optimization for 99 % energy efficiency with six reactants (A)-(F).

Iter.	572	573	574	575	576
f_{x_2} , mm	10.6	10.5	9.6	9.6	9.4
f_{y_2} , mm	-22.1	-22.1	-22.2	-22.2	-22.1
v_{x_2} , mm	-21.7	-22.1	-21.9	-21.8	-21.8
v_{y_2} , mm	4.5	4.4	4.2	4.2	4.1
d_2 , mm	92.8	93.0	92.5	92.4	92.5
s_2 , mm	95.2	95.0	94.9	94.9	95.1
D_2 , mm	250.6	250.2	249.6	249.6	249.6

With only a 64-point DB required to find the geometry of a 97.5% efficient reactor, in another test we attempt the more challenging task of finding the optimal solution for $T = 1$ %. By applying this more tough constraint (and simultaneously keeping the bandwidth goal values set to 100%), we are interested in seeing the capability of the optimization technique in searching for an optimal solution with bigger BW_r . Here, an initial DB, also, contains 50 points for each of the six reactants. The “best” optimal solution producing 99 % efficiency is $BW_r^A = 80\%$, $BW_r^B = 79\%$, $BW_r^C = 91\%$, $BW_r^D = 79\%$, $BW_r^E = 95\%$, and $BW_r^F = 97\%$, and it is achieved with 527 DB points requiring 3,456 FDTD simulations. Graphs in Fig. 13 show the natural effect of quicker convergence for the reactants with higher loss factors ((E) and (F)) than with a lower one (B). Corresponding design variables are given in the last column of Table 4 which also shows how the “best” optimal solution was finally approached in the course of optimization. Frequency characteristics of $|S_{11}|$ resulting from the 576th solution are shown in Fig. 14: for all the reactants (A)-(F), this configuration provides 99 % efficiency in the 79 % of the 2.4 to 2.5 GHz frequency range.

V. CONCLUSION

In this paper, we have introduced an original modeling-based approach for CAD and scaling up of MAOS reactors. A computer code implementing the proposed technique allows for finding the geometry of a large-scale reactor that guarantees the highest possible energy efficiency for different reactants. The procedure of RBF ANN optimization backed by full-wave (3D conformal FDTD) simulations has been applied to a conventional MW reactor to find the best design for processing of 1- and 5-liter reactants. It has been demonstrated that, with the developed technique, seven-parameter optimization of this system that aims to guarantee 99 % efficiency takes only 297 and 195 FDTD analyses (i.e., about 16 and 37.5 h of CPU time of a regular PC), respectively. The optimization technique remains operational and viable when it is used for a larger number of materials – e.g., it requires 3,456 simulations when working

with the same seven design variables for six different reactants.

The advanced functionality of the presented optimization technique is eloquently illustrated by the output of our earlier paper [20] showing, with the use of the technique [16], that a MW applicator optimized for only one load may behave unsatisfactorily for the other ones. On the other hand, our RBF optimization procedures are straightforwardly applicable to those systems with loads whose material parameters strongly depend on temperature. This has been already shown, in a simplified manner, in [21] where the technique [16] was applied to loads with different values of uniformly distributed complex permittivity. In a more accurate way, the temperature dependence can be handled by the optimization technique described in this paper if it is backed by *QW-3D* which provides a regime of operating the FDTD solver with a cell-by-cell modification of media parameters as a function of dissipated power.

The results, presented in this paper, stay in strong favor of CAD of high-productive large-scale MAOS reactors and suggest that application of the developed modeling-based optimization procedure in efficient designing of systems of MW chemistry may be useful and practical.

REFERENCES

- [1] P. Lidstrom, J. Tierney, B. Wathey, and J. Westman, “Microwave assisted organic synthesis – a review,” *Tetrahedron*, vol. 57, pp. 9225-9283, 2001.
- [2] D. Bodgal, *Microwave-Assisted Organic Synthesis*, Elsevier, 2005.
- [3] C. O. Kappe and A. Stadler, *Practical Microwave Synthesis for Organic Chemists: Strategies, Instruments, and Protocols*, Wiley-VCH, 2009.
- [4] J. M. Kremsner, A. Stadler, and C. O. Kappe, “The scale-up of microwave-assisted organic synthesis,” *Top Curr Chem*, vol. 266, pp. 233-278, 2006.
- [5] V. V. Komarov and V. V. Yakovlev, “CAD of efficient TM_{m0} single-mode elliptical applicators with coaxial excitation,” *J. Microwave Power & Elec-tromag. Energy*, vol. 40, no. 3, pp. 174-185, 2007.
- [6] M. Celuch, W. K. Gwarek, and M. Sypniewski, “A novel FDTD system for microwave heating and thawing analysis with automatic time-variation of enthalpy-dependent media parameters,” *Advances in Microwave and Radio-Frequency Processing*, pp. 199-207, 2006.
- [7] P. Kopyt and M. Celuch, “Coupled electromagnetic thermodynamic simulations of microwave heating

- problems using the FDTD algorithm,” *J. Microwave Power & Electromag. Energy*, vol. 41, no. 1, pp. 18-29, 2007.
- [8] M. Celuch and P. Kopyt, “Modeling microwave heating of food,” *Development of Packaging and Products for Use in Microwave Ovens*, pp. 307-350, 2009.
- [9] V. A. Mechenova and V. V. Yakovlev, “Efficiency optimization for systems and components in microwave power engineering,” *J. Microwave Power & Electromag. Energy*, vol. 39, no. 1, pp. 15-29, 2004.
- [10] B. G. Cordes and V. V. Yakovlev, “Computational tools for synthesis of a microwave heating process resulting in the uniform temperature field,” *Proc. 11th AMPERE Conf. Microwave and High Frequency Heating*, pp. 71-74, September 2007.
- [11] E. E. Eves, B. G. Cordes and V. V. Yakovlev, “Modeling-based synthesis of a microwave heating process producing homogeneous temperature field,” *Proc. 24th Annual Review of Progress in Applied Computational Electromagnetics*, pp. 542-544, 2008.
- [12] S. Kalhori, N. Elander, J. Svennebrink, and S. Stone-Elander, “A re-entrant cavity for microwave-enhanced chemistry,” *J. Microwave Power & Electromag. Energy*, vol. 38, no. 2, pp. 125-135, 2004.
- [13] K.-M. Huang, Z. Lin, and X.-Q. Yang, “Numerical simulation of microwave heating of chemical reaction in dilute solution,” *Progress in Electromagnetics Research (PIER)*, vol. 49, pp. 273-289, 2004.
- [14] E. K. Murphy and V. V. Yakovlev, “RBF network optimization of complex microwave systems represented by small FDTD modeling data sets,” *IEEE Trans. Microwave Theory Tech.*, vol. 54, no. 7, pp. 3069-3083, 2006.
- [15] H. Kabir, Y. Wang, M. Yu, and Q. J. Zhang, “Neural network inverse modeling and applications to microwave filter design,” *IEEE Trans. Microwave Theory and Tech.*, vol. 56, no. 4, pp. 867-879, 2008.
- [16] E. K. Murphy and V. V. Yakovlev, “Reducing a number of full-wave analyses in RBF neural network optimization of complex microwave structures,” *IEEE MTT-S Intern. Microwave Symp. Dig.*, pp. 1253-1256, June 2009.
- [17] H. Kabir, Y. Wang, M. Yu, and Q. J. Zhang, “Advances of neural network modeling methods for RF/microwave applications,” *ACES Journal*, vol. 25, no. 5, pp. 423-432, 2010.
- [18] R. G. Regis and C. A. Shoemaker, “Constrained global optimization of expensive black box functions using radial basis functions,” *J. Global Optim.*, vol. 31, no. 1, pp. 153-171, 2005.
- [19] *QuickWave-3D*, QWED, <http://www.qwed.com/pl>, 1997-2009.
- [20] E. K. Murphy and V. V. Yakovlev, “RBF network optimization with CORS sampling for practical CAD of microwave applicators,” *Proc. 12th AMPERE Conf. Microwave and High Frequency Heating*, pp. 79-82, September 2009.
- [21] E. K. Murphy and V. V. Yakovlev, “Efficiency optimization for microwave thermal processing of materials with temperature-dependent media parameters,” *Proc. Progress in Electromagnetics Research Symp.*, pp. 400-401, August 2009.



Ethan K. Murphy received the M.S. degree in Industrial Mathematics from Worcester Polytechnic Institute (WPI), Worcester, MA in 2003 and the Ph.D. degree in Mathematics from Colorado State University,

Fort Collins, CO in 2007. He then held two post-doc positions – at the WPI’s Department of Mathematical Sciences (2008-2009) and at the Department of Biomedical Engineering at Rensselaer Polytechnic Institute, Troy, NY (2009-2010). He is currently with Applied Mathematics, Inc. His research interests include inverse problems, microwave optimization, microwave imaging, diffuse optical tomography, and electric impedance tomography. He has authored more than 20 papers in referred journals and conference proceedings. Dr. Murphy is a member of the American Mathematical Society and Pi Mu Epsilon.



Vadim V. Yakovlev received his Ph.D. degree in Radio Physics from the Institute of Radio Engineering and Electronics (IRE) of the Russian Academy of Sciences (RAS), Moscow, Russia in 1991. From 1984 to 1996, he

was with IRE RAS as Junior Research Scientist, Research Scientist, and Senior Research Scientist. In 1993, he worked as Visiting Researcher at Electricité de France (Centre “Les Renardières”).

In 1996, he joined the Department of Mathematical Sciences, Worcester Polytechnic Institute, Worcester, MA and currently holds there a position of Research Associate Professor. Dr. Yakovlev is a head of the Industrial Microwave Modeling Group which he established in 1999 as a division of the WPI’s Center for Industrial

Mathematics and Statistics. Dr. Yakovlev's research interests in computational electromagnetics include neural-network-based optimization, microwave imaging, multiphysics modeling, microwave power engineering, and broadband/multiband antennas. He is an author of more than 120 papers in referred journals and conference proceedings. Dr. Yakovlev is a senior member of the IEEE, a member of the Technical Advisory Board of International Microwave Power Institute (IMPI), a member of Association for Microwave Power in Europe for Research and Education (AMPERE) and a member of the Massachusetts Institute of Technology (MIT) Electromagnetics Academy. He serves as a reviewer for several journals and as a member of program committees of several conferences.